

Chapter 1

Introduction

Particle physics deals with the study of the basic constituents of matter and the forces governing the interactions among them. The Standard Model (SM) is the most accepted theory describing the nature and properties of the fundamental particles and their interactions. The elementary particles leptons and quarks, known as fermions, interact through the exchange of the gauge bosons. The gauge bosons acquire masses in the process of electroweak symmetry breaking whereas the masses of the fermions are generated through Yukawa interactions with the field associated to the scalar Higgs boson. The gauge bosons are the mediators of the four fundamental forces of interaction existing in nature : the electromagnetic force, the strong force, the weak force and the gravitational force. Quantum Chromodynamics (QCD) is the theory of the strong interactions between the quarks mediated by the massless gluons. The quarks and gluons, together known as partons, have a peculiar property of “color” charge. Due to confinement property of QCD, the quarks cannot exist freely in nature but bind themselves into colorless particles called hadrons such as protons and neutrons together known as nucleons, pions etc. The structure and the properties of sub-atomic particles can be explored by first accelerating them using particle accelerators and then colliding at very high energies. The end products of these collisions are recorded in the ~~real~~ particle detectors constituting the real data.

*slang
measurements?*

Vorlesung
 $\text{pp} \rightarrow i\text{jets} + X$, is proportional to α_s^i . The study of inclusive jet cross-sections in terms of jet transverse momentum p_T and rapidity y is very important because it provides the essential information about the PDFs and the precise measurement of α_s . Also the ratio of cross-sections given by Eq. 1.1 is proportional to the QCD coupling constant α_s and hence can be used to determine the value of α_s .

$$R_{mn} = \frac{\sigma_{m-jet}}{\sigma_{n-jet}} \propto \alpha_s^{m-n} \quad (1.1)$$

Instead of studying inclusive cross-sections, the cross-section ratio is more useful because of the partial or complete cancellation of many theoretical and experimental uncertainties in the ratio. The CMS Collaboration has previously measured the ratio of the inclusive 3-jet cross-section to that of the inclusive 2-jet as a function of the average transverse momentum, $\langle p_{T1,2} \rangle$, of the two leading jets in the event at 7 TeV [1]. This study leads to an extraction of $\alpha_s(M_Z) = 0.1148 \pm 0.0055$, where the dominant uncertainty stems from the estimation of higher-order corrections to the next-to-leading order (NLO) prediction. In this thesis, a measurement of inclusive 2-jet and 3-jet event cross-sections as well as ratio of 3-jet event cross-section over 2-jet R_{32} , is performed using an event sample collected during 2012 by the CMS experiment at the LHC and corresponding to an integrated luminosity of 19.7 fb^{-1} of pp collisions at a center-of-mass energy of 8 TeV. The event scale is chosen to be the average transverse momentum of the two leading jets, referred to as $H_{T,2}/2$

*Unclear:
 It is predicted
 if known
 at one
 scale, e.g. M_Z*
 in this thesis. The strength of the strong force, α_s at a given energy scale Q is not predicted and has to be extracted from the experiment. Hence, the value of the strong coupling constant at the scale of the Z boson mass $\alpha_s(M_Z)$ is extracted from the measurements performed in this thesis. The value of α_s depends on the energy scale Q and it decreases with the increase of Q scale. The running of α_s with scale Q is also studied and compared with other CMS measurements as well as results from different experiments. This checks the consistency with QCD via the

Chapter 7 describes the method to extract the strong coupling constant at the scale of mass of Z boson $\alpha_s(M_Z)$ from the measurements of differential inclusive multijet cross-sections and the cross-section ratio R_{32} . Also, the running of α_S with energy scale Q is presented along with the previous measurements from different experiments.

Chapter 8 summarizes the results and conclusions of the work done in this thesis.

Chapter 9 mentions the participation in other hardware and software activities.

Chapter 2

Theoretical Background

Since 1930s, many theories and discoveries in particle physics have revealed the fundamental structure of matter. The matter is made up of fundamental particles and their interactions are mediated by four fundamental forces [2]. The theoretical models describe all the phenomena of particle physics as well as predict the properties of particles. These models must be either confirmed experimentally or totally excluded giving hints of new physics. This interplay between experimental discoveries and the corresponding theoretical predictions leads to a theoretical model called Standard Model, which describes the fundamental particles and their interactions. The world's most powerful particle accelerators and detectors are used by physicists to test the predictions and limits of the Standard Model where it has successfully explained almost all experimental results. This chapter describes the Standard Model with main focus on the theory of strong interactions called Quantum Chromodynamics and its features which serve as the theoretical base of this thesis.

maybe? strive to describe, masses are not predicted

2.1 Standard Model

The Standard Model (SM) of particle physics [3–5] was developed in 1970s. It is a mathematical framework which describes the nature and properties of the funda-

Depending on how the fermions interact, these are classified into two categories - leptons (ℓ) and quarks (q). The leptons are of six types : electron (e), muon (μ) and tau (τ) with electric charge $Q = \pm 1$ ⁴ and the corresponding neutrinos : electron neutrino (ν_e), muon neutrino (ν_μ) and tau neutrino (ν_τ) having electric charge $Q = 0$. The quarks exist in six “flavors” : up (u), down (d), strange (s), charm (c), bottom (b) and top (t). u , c and t carry electric charge $Q = \pm \frac{2}{3}$ whereas d , s and b carry $Q = \pm \frac{1}{3}$. The quarks and leptons are categorized into three generations. The first generation has the lightest and the most stable particles whereas the heavier and less stable particles belong to the second and third generations.

The elementary bosons have integral spin and obey the Bose-Einstein statistics. These are further of two types : gauge bosons having non-zero integral spin and a scalar boson with zero spin. The gauge bosons are the force carriers which mediate the electromagnetic, strong, weak and gravitational forces. Every interaction involves the exchange of a gauge boson : the massless photon (γ) for the electromagnetic force, massless gluons (g) for the strong force, massive W^\pm and Z for the weak force and the graviton (not yet found) for the gravitational force. However, the gravitational force has not been incorporated into SM yet. Along with this, the existence of dark matter or dark energy and the matter-antimatter asymmetry are still missing pieces in the SM. The interaction between fundamental particles acts because of some peculiar property of the particles - charge for the electromagnetic force, color for the strong force and flavor for the weak force. *Usually Beyond SM.*

In the SM, the forces of interaction except gravity are unified into one quantum field theory [6], known as Grand Unified Theory (GUT) [7–9]. The SM framework based on quantum field theories is described by $SU(3)_C \otimes SU(2)_L \otimes U(1)_Y$ gauge symmetry where C stands for the color charge, L for weak isospin and Y for hypercharge. Here $SU(3)_C$, $SU(2)_L$ and $U(1)_Y$ terms give rise to strong, weak and

*Undefined
 $Y = ?$
Where is Q^3 ?*

⁴ all charges are expressed in units of elementary charge e

Define together with $t=c=1$?

Similar

has a same role as the electric charge in electromagnetic interactions. However, the mediator of electromagnetic interactions i.e. the photon itself does not carry any electric charge whereas the gluon itself carry color charge. This allows the self coupling of gluons and hence makes the theory non-abelian. Both the quarks and gluons carry three types of color charges : red (r), green (g) and blue (b), and three types of anti-color charges : anti-red (\bar{r}), anti-green (\bar{g}) and anti-blue (\bar{b}). The quarks carry a single color charge whereas gluons carry a combination of color charges. There are nine eigen states of gluons but one of them $\frac{1}{\sqrt{3}}(r\bar{r} + g\bar{g} + b\bar{b})$ is a totally symmetric color singlet which has no net color charge and does not take part in interaction.

The remaining eight eigen states of the gluons are :

$$r\bar{b}, r\bar{g}, g\bar{r}, g\bar{b}, b\bar{g}, b\bar{r}, \frac{1}{\sqrt{2}}(r\bar{r} - b\bar{b}), \frac{1}{\sqrt{6}}(r\bar{r} + b\bar{b} - 2g\bar{g}) \quad (2.1)$$

The dynamics of the quarks and gluons are controlled by the gauge invariant QCD Lagrangian \mathcal{L}_{QCD} which is composed of four terms as :

$$\mathcal{L}_{QCD} = \underbrace{-\frac{1}{4}F_{\mu\nu}^A F_A^{\mu\nu}}_{\mathcal{L}_{gluons}} + \underbrace{\sum_{flavors} \bar{q}_a (i\gamma^\mu (D_\mu)_{ab} - m_q) q_b}_{\mathcal{L}_{quarks}} + \mathcal{L}_{gauge} + \mathcal{L}_{ghost} \quad (2.2)$$

where \mathcal{L}_{gluons} describes the kinetic term of the gluon fields A_μ^A ; \mathcal{L}_{quarks} defines the interaction between spin- $\frac{1}{2}$ quark fields q_a of mass m_q and spin-1 gluon fields A_μ^A summing over all presently known six flavors of quarks; \mathcal{L}_{gauge} describes the chosen gauge and \mathcal{L}_{ghost} is the so-called ghost term required to treat the degeneracy of equivalent gauge field configurations in non-abelian gauge theories. In Eq. 2.2, the Greek letters $\mu, \nu, \dots \in \{0,1,2,3\}$ are the space-time indices; $a,b,c \in \{1,2,3\}$ and $A,B,C \in \{1,\dots,8\}$ are the indices of the triplet and octet representations, respectively,

color

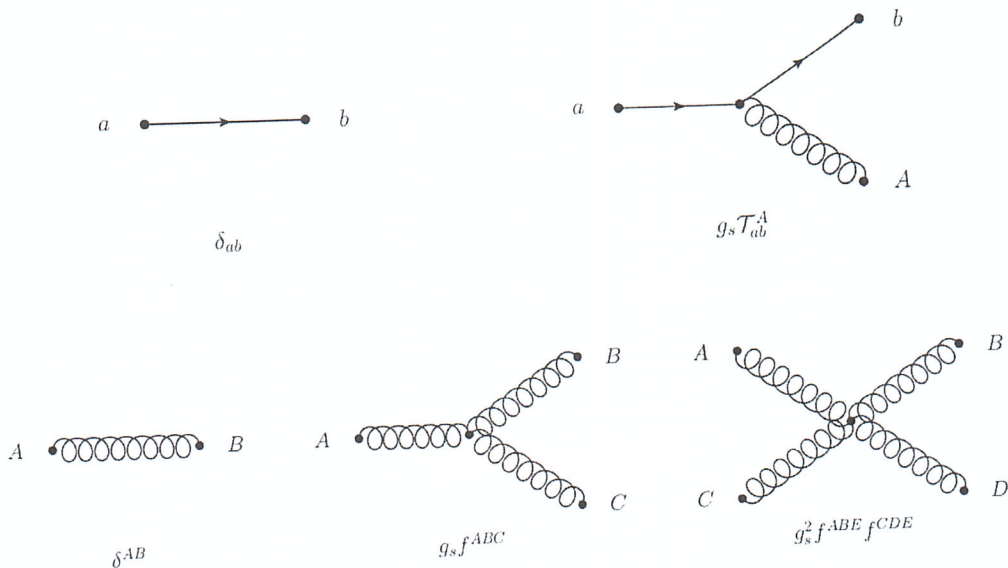


Figure 2.2: The fundamental Feynman rules of a free quark-field term (top left), cubic quark-gluon interaction term (top right), free gluon-field term (bottom left), quartic gluon self-interaction term (bottom middle) and quartic gluon self-interaction term (bottom right). Taken from [17].

is given by

$$\mathcal{L}_{gauge} = -\frac{1}{2\xi} (\partial^\mu \mathcal{A}_\mu^A)^2 \quad (2.6)$$

where ξ may be any finite constant. This choice fixes the class of covariant gauges with ξ as the gauge parameter. As QCD is non-abelian, the gauge fixing term must be supplemented by a ghost Lagrangian as

$$\mathcal{L}_{ghost} = \partial_\alpha \eta^{A\dagger} (D_{AB}^\mu \eta^B) \quad (2.7)$$

where η^A is a complex scalar field which obeys Fermi-Dirac statistics. The ghost fields cancel unphysical degrees of freedom arising due to use of covariant gauges. This completes the QCD Lagrangian shown in Eq. 2.2.

The strength of an interaction is given by a fundamental parameter called the coupling constant α . In QED, the coupling constant $\alpha_e = e^2/4\pi = 1/137$ is constant. In contrast to this, in QCD, the coupling constant $\alpha_s(Q) = g_s^2/4\pi$ is

No, also α_e is running because of renormalisation!

e.g.: $\alpha_e(M_Z) \approx 1/128$

to that process. For a given Feynman diagram, the power of α_s is determined by the number of vertices associated with quark-gluon or gluon-gluon interactions. A leading order (LO) prediction sums over only the lowest-order contribution whereas next-to-leading order (NLO) includes terms with ~~the additional powers~~^{one} of α_s . The next-to-next-to-leading order (NNLO) includes emission of another gluon or a virtual gluon loop. The different order of the QCD processes are shown in Fig. 2.3. The calculations become complex with the loop diagrams where the momenta of

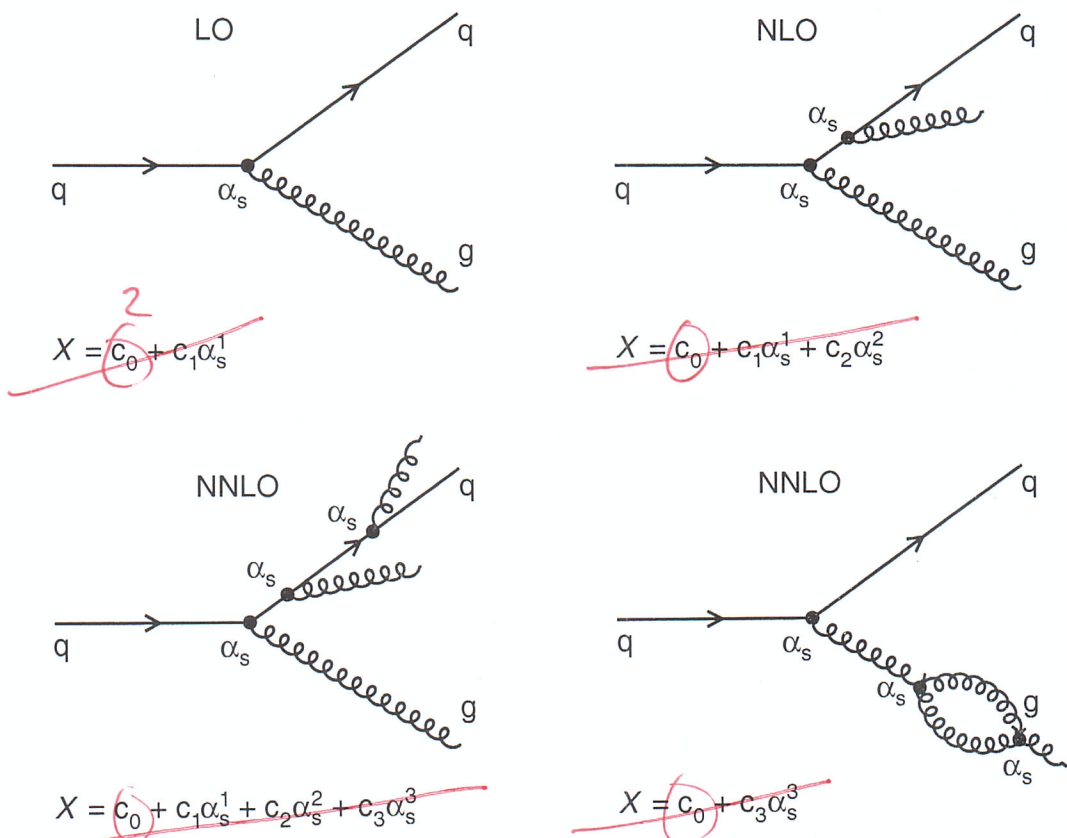


Figure 2.3: ~~The~~⁵ Feynman diagrams⁵ of leading-order (LO), next-to-leading order (NLO) and next-to-next-to-leading order (NNLO) processes in quantum chromodynamics along with the perturbative expansion of any observable X in powers of the strong coupling constant α_s . At each successive step in perturbation series, the emission of an additional gluon take place.

Power counting not clear. Better show concrete diagrams for your case. See after page 31!

the virtual particles in a loop are not fully constrained by four-momentum conservation and the associated integrals are divergent. Such ultraviolet (UV) divergences

⁵Drawn using ROOT

By setting the renormalization scale equal to the physical scale i.e. $\mu^2 = Q^2$, $X(1, \alpha_s(Q))$ is a solution to above equation. Q -dependence of ~~the~~ X is only from the renormalization of the theory which is present in the ~~classical~~? theory. Hence measuring the Q -dependence of X will directly probe the quantum structure of the theory. The β function in QCD has a perturbative expansion as :

$$\beta(\alpha_s) = -\alpha_s^2 \left(b_0 + b_1 \alpha_s + b_2 \alpha_s^2 + \mathcal{O}(\alpha_s^3) \right) \quad (2.11)$$

where b_n is the $n+1$ -loop β -function coefficients giving the dependence of the coupling on the energy scale Q . In the modified minimal subtraction ($\overline{\text{MS}}$) scheme [19, 20], the beta coefficient functions have following values :

$$b_0 = \frac{33 - 2n_f}{12\pi}, \quad b_1 = \frac{153 - 19n_f}{24\pi^2}, \quad b_2 = \frac{77139 - 15099n_f + 325n_f^2}{3456\pi^3} \quad (2.12)$$

where n_f is the number of quark flavours with masses $m_q < \mu_r$. On integration of Eq. 2.11, the energy dependence of α_s is yielded. Neglecting the higher orders, the first order solution of RGE is :

$$\alpha_s(\mu_r^2) = \frac{1}{b_0 \ln(\mu_r^2/\Lambda_{QCD}^2)} \quad (2.13)$$

where Λ_{QCD} is the constant of integration. The perturbative coupling becomes large at the scale Λ_{QCD} and the perturbative series diverge. With $b_0 > 0$, the coupling becomes weaker at higher scales Q , i.e. the effective color charge is small at small distances or large energies. This allows the quarks to behave as free particles within the hadron, leading to the property called asymptotic freedom. It is always convenient to express α_s at some fixed scale. Since some of the best measurements come from Z decays, it is common practise to determine the strong coupling at the $\overline{c^2}$.

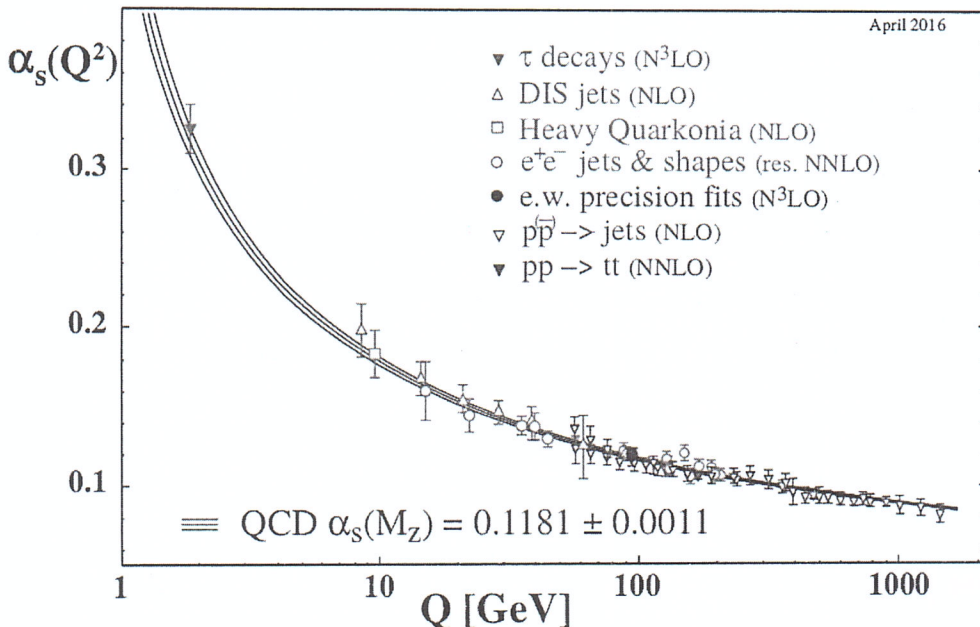


Figure 2.4: The different experimental measurements of the strong coupling constant α_S evolved at the energy scale Q are shown as a function of Q . These describe the running of the α_S up to the 1 TeV scale. Taken from [21].

final state?

specific process. In a hadronic collision, the perturbation theory is only valid at the parton-level but due to property of confinement at low energies, free partons cannot exist in nature. Only hadrons with a complex internal structure are available for the high energy collisions. Here, a factorization theorem of QCD [22] comes into play which allows the calculation of σ by separating into two parts : a short-distance partonic cross-section calculable with pQCD, and a non-perturbative long-distance part described by parton distribution functions $f_i(x, \mu_f)$ (PDFs). The PDFs describe the partonic content of the colliding hadrons and give the probability to find a parton i with momentum fraction x within a hadron. μ_f is a factorization scale which corresponds to the resolution with which the hadron is being probed. The particles which are emitted with transverse momenta $p_T > \mu_f$ are considered in the calculation of hard scattering perturbative coefficients. The particles emitted with $p_T < \mu_f$ are accounted for within the PDFs. Applying the factorization theorem

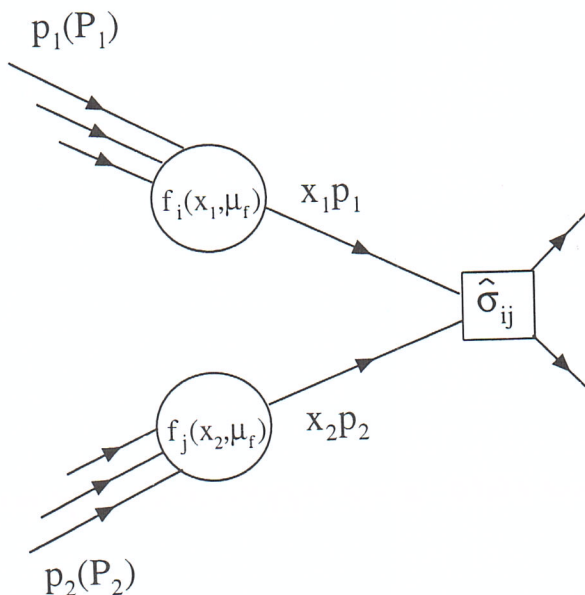


Figure 2.5: Schematic illustration⁶ of the factorization theorem in a collision of two protons P_1 and P_2 having momenta p_1 and p_2 , respectively. In a hard-scattering process at a scale Q^2 , the two partons x_1 and x_2 participate with momenta $x_1 p_1$ and $x_2 p_2$. The total cross-section is factorized into the hard scattering cross-section $\hat{\sigma}_{ij}$ calculable using perturbative quantum chromodynamics and the PDFs $f_i(x_1, \mu_f)$ and $f_j(x_2, \mu_f)$ with factorization scale μ_f .

p QCD

2.3.1 Parton Shower and Hadronization

The partons involved in a hard scattering process get accelerated due to large momentum transfers. These accelerated partons emit QCD radiation in the form of gluons with successively lower energy. Unlike the uncharged photons in QED, the gluons themselves carry color charge and hence also emit further gluons. The emitted gluons in turn split into $q\bar{q}$ pairs. This successive emission of partons leads to a parton shower. In a parton shower, the main contribution is by the collinear parton splitting and the soft gluon emissions. The parton showers mimic the effect of higher-order corrections to the hard process. These cannot be calculated exactly and are taken into account using the parton shower approximation. The two incom-

*Unity
color
vs.
colour
usage.*

⁶Drawn using ROOT

A consequence

Due to this, the potential energy of the string grows at the expense of the kinetic energy of the quarks. As the potential energy becomes of the order of hadron masses, the string breaks at some point along its length, creating a new $q\bar{q}$ pair. The newly formed two string segments again stretch and break producing further $q\bar{q}$ pairs. This process of stretching and breaking continues until all the potential energy gets converted to $q\bar{q}$ pairs. This whole process is illustrated in Fig 2.6. The $q\bar{q}$ pairs then undergo hadronization due to confinement property. PYTHIA Monte Carlo generator uses the Lund string model.

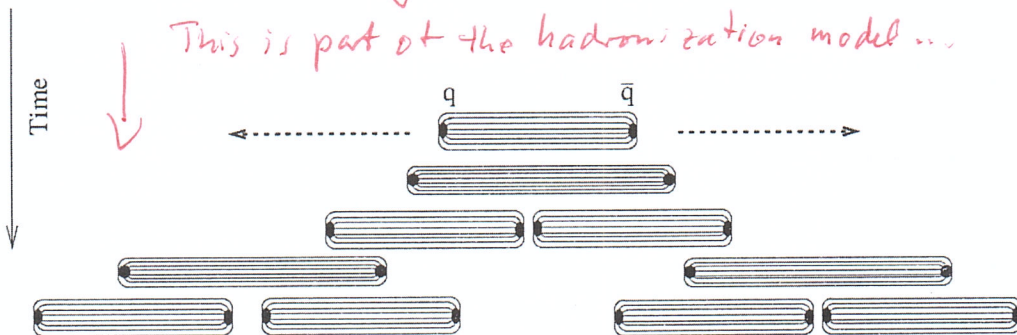


Figure 2.6: Illustration of the hadronization process in Lund string model⁸. When the quark q and anti-quark \bar{q} are pulled apart from each other, the potential energy of the gluonic string connecting the quarks increases. As it becomes of the order of hadron masses, the string breaks and a new $q\bar{q}$ pair is created. The breaking of string and creation of $q\bar{q}$ continues till all the potential energy gets converted to $q\bar{q}$ pairs which then get hadronized.

Cluster Model - The cluster model of hadronization [33, 34] is based on preconfinement property of QCD [35]. According to this property, at evolution scales Q_0 much less than the hard process scale Q , the partons produced in a shower are clustered in colourless groups with an invariant mass distribution, depending on nature of hard process and Q_0 , not on Q . This model contains two steps : firstly all gluons split into $q\bar{q}$ pairs at the end of the parton shower and in the second step, a new set of low-mass color-singlet clusters are obtained which decay into either secondary clusters or directly into hadrons. The generator HERWIG is based on the cluster

⁸Source : <http://inspirehep.net/record/806744>

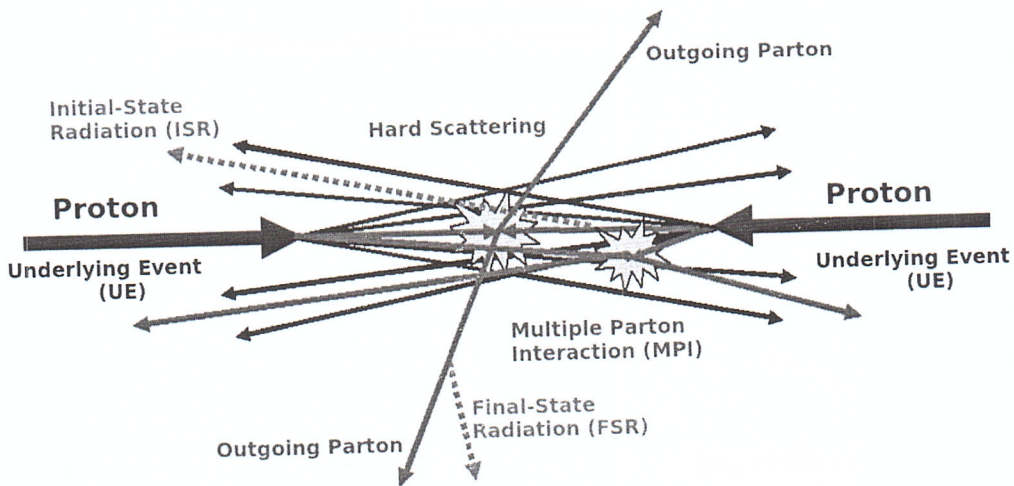


Figure 2.7: A proton-proton collision⁹ involving the main hard scattering process along with the low momentum transfer underlying event (UE) contributions coming from initial- and final-state radiations (ISR and FSR) complemented with multiple parton interactions (MPI) and collisions from leftover partons called beam remnants.

At the

and also to reduce the uncertainties of the PDFs of proton. In LHC, the simplest jet production process is $2 \rightarrow 2$ scattering process at leading-order giving dijet events. But the partons originating from ISR, FSR or MPI can also hadronize to produce jets greater than 2 in a single proton-proton collision. This results in the production of multijet events. The investigation of inclusive multijet event cross-sections permits more elaborate tests of QCD. Also, a precise study of jet variables helps to understand the signal and background modelling for the new physics searches in hadronic final states. In this thesis, the inclusive multijet event cross-sections as well as the ratio of cross-sections are exploited to extract the value of strong coupling constant α_s . In the next section, we focus on the definition of a jet.

In your analysis the UE multijet events are cut out using $P_T > 100 \text{ GeV}$.

2.4 Jets

Jets [36] are the conical structures which group the hadrons into a single physics entity. Figure 2.8 shows the the outgoing partons of the hard scattering process

⁹Source : The Energy Dependence of Min-Bias and the Underlying Event at CDF

This is not
the
point!
Only at
low P_T !!
Then jets
are back
ground.
The real
multijet
is from
 $2 \rightarrow 3$
 $2 \rightarrow 4$
...
parton
reaction!
in QCD!

ated with a jet algorithm which calculates the momentum assigned to the combined particles. A jet algorithm along with its parameters and a recombination scheme forms a “jet definition”. A jet definition [39] must be simple to implement in an experimental analysis as well as in the theoretical calculation. It should be defined at any order of perturbation theory and must yield finite cross-sections that is relatively intensive to hadronization. In addition to these requirements, a jet algorithm must be infrared and collinear (IRC) safe. Infrared safety is the property by which the addition of a soft emission i.e. addition of a soft gluon should not change or modify the number of hard jets found in an event. In an infrared unsafe algorithm, a soft gluon emission in the middle of two cone jets can lead to overlap of the two initial cones, as shown in Fig. 2.9 (top). This produces a single jet instead of initial

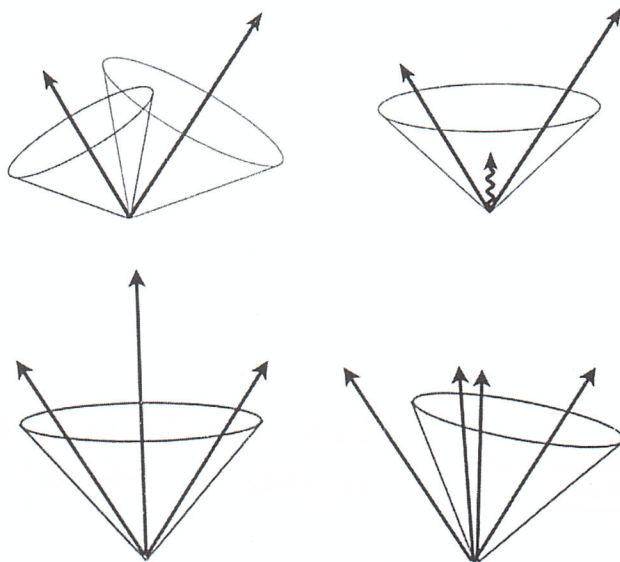


Figure 2.9: Top : Infrared unsafe behaviour of jet algorithm is illustrated where the presence of soft radiation between two jets may cause a merging of the jets that would not occur in the absence of the soft radiation. Bottom : Collinear unsafe behavior of jet algorithm is shown in which the number of jets change due to a collinear splitting¹⁰.

two jets resulting in the change of number of jets. Collinear safety is the property by virtue of which the collinear splitting i.e. replacement of one parton by two at

¹⁰Source : <http://inspirehep.net/record/1251416>

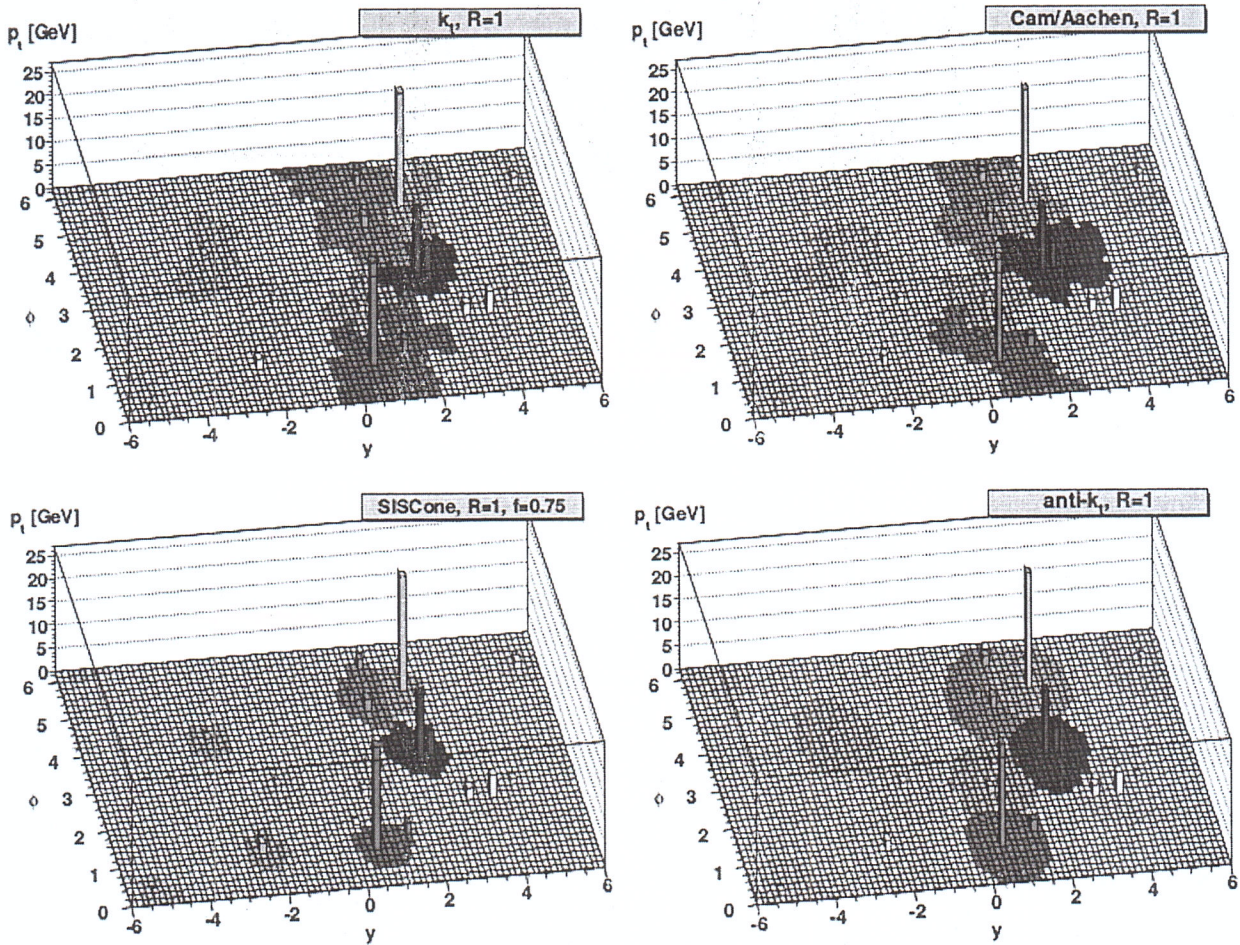


Figure 2.10: The clustering of particles, in $y\phi$ space at the parton level, into jets clustered with the k_t (top left), Cambridge/Aachen (top right), SIScone (bottom left) and anti- k_t (bottom right) algorithms with $R = 1$. The towers represent the jet p_T . The anti- k_t algorithm gives circular jets while the jets produced with other three algorithms have irregular shapes. Taken from [38].

corresponds to vector addition of four-momenta where the four-momenta of the jet is obtained by simply adding the four-momenta vector of merging particles.

The sequential clustering algorithms have ~~always~~ been favoured by theorists but not by experimentalists because of slow computational performance. However, the introduction of the FASTJET program [47] enhanced the speed of clustering algorithms and hence are preferred by experimentalists as well. This thesis studies the particles produced in proton-proton collisions by clustering them in to jets using

anti- k_t algorithm with distance parameter $R = 0.7$. These jets are observed in the Compact Muon Solenoid detector of the Large Hadron Collider, the details of which are discussed in the following chapter.